

Applications of Hierarchical Cluster Analysis (CLA) and Principal Component Analysis (PCA) in Feed Structure and Feed Molecular Chemistry Research, Using Synchrotron-Based Fourier Transform Infrared (FTIR) Microspectroscopy

PEIQIANG YU*

College of Agriculture, University of Saskatchewan, 51 Campus Drive,
 Saskatoon, Saskatchewan, Canada S7N 5A8

Synchrotron technology based Fourier transform infrared microspectroscopy (S-FTIR) is a recently emerging bioanalytical microprobe capable of exploring the molecular chemistry within microstructures of feed tissues at a cellular or subcellular level. To date there has been very little application of hierarchical cluster analysis (CLA) and principal component analysis (PCA) to the study of feed inherent microstructures and feed molecular chemistry between feeds and/or between different structures within a feed, in relation to feed quality and nutrient availability using S-FTIR. In this paper, multivariate statistical methods—CLA and PCA—were used to analyze synchrotron-based FTIR individual spectra obtained from feed inherent microstructures within intact tissues by using the S-FTIR as a novel approach. The S-FTIR spectral data of three feed inherent structures (structure 1, feed pericarp; structure 2, feed aleurone; structure 3, feed endosperm) and different varieties of feeds within cellular dimensions were collected at the National Synchrotron Light Source (NSLS) at Brookhaven National Laboratory (BNL), U.S. Department of Energy (NSLS-BNL, New York). Both PCA and CLA methods gave satisfactory analytical results and are conclusive in showing that they can discriminate and classify inherent structures and molecular chemistry between and among the feed tissues. They also can be used to identify whether differences exist between the varieties. These statistical analyses place synchrotron-based FTIR microspectroscopy at the forefront of those new potential techniques that could be used in rapid, nondestructive, and noninvasive screening of feed intrinsic microstructures and feed molecular chemistry in relation to the quality and nutritive value of feeds.

KEYWORDS: Principal component analysis; cluster analysis; feed structures; feed molecular chemistry; synchrotron FTIR microspectroscopy

INTRODUCTION

Synchrotron technology (*1*) based Fourier transform infrared microspectroscopy (S-FTIR) is a recently emerging bioanalytical microprobe. This analytical technique is capable of exploring the molecular chemistry within microstructures of a biological tissue and providing high signal-to-noise ratio spectra at high spatial resolutions (cellular or subcellular level) (*2–5*). Very recently, this technique has been used in feed science, feed molecular chemistry, feed structural biology, and animal nutrition research (*6–11*). The S-FTIR technique, taking advantage of synchrotron light brightness (*3, 12, 13*), is able to provide four types of information simultaneously: tissue composition, tissue environment, tissue structure, and tissue chemistry (*14*).

The most straightforward method of S-FTIR spectral data analysis is the checking of specific functional group intensities and frequencies associated with the chemical constituents of a

feed (e.g., protein amide I, $\sim 1650\text{ cm}^{-1}$, and protein amide II, $\sim 1550\text{ cm}^{-1}$; lipid C=O carbonyl ester, $\sim 1740\text{ cm}^{-1}$; lignin aromatic compound, $\sim 1515\text{ cm}^{-1}$) by peak heights and/or areas (*13, 15*). However, this univariate statistical approach (*13, 15*) does not always accurately identify functional group location and concentration.

Hierarchical cluster analysis (CLA) and principal component analysis (PCA) are two multivariate analyses that could be used for IR spectrum analysis (*13, 15*). However, to date there has been very little application of CLA and PCA to the study of feed inherent microstructures and feed molecular chemistry at a cellular level. These inherent structure and molecular chemical characteristics are highly associated with feed quality, nutritive value, and nutrient utilization (*7, 8, 11*).

The objective of this study was to use CLA and PCA to analyze synchrotron-based FTIR individual spectra (C_P IR group, C_E IR group, and B_E IR group) obtained, respectively, from various feed inherent structures (feed structure 1, pericarp; structure 2, aleurone; structure 3, endosperm) and different

* Telephone (306) 966-4132; fax (306) 966-4151; e-mail: yupe@sask.usask.ca.

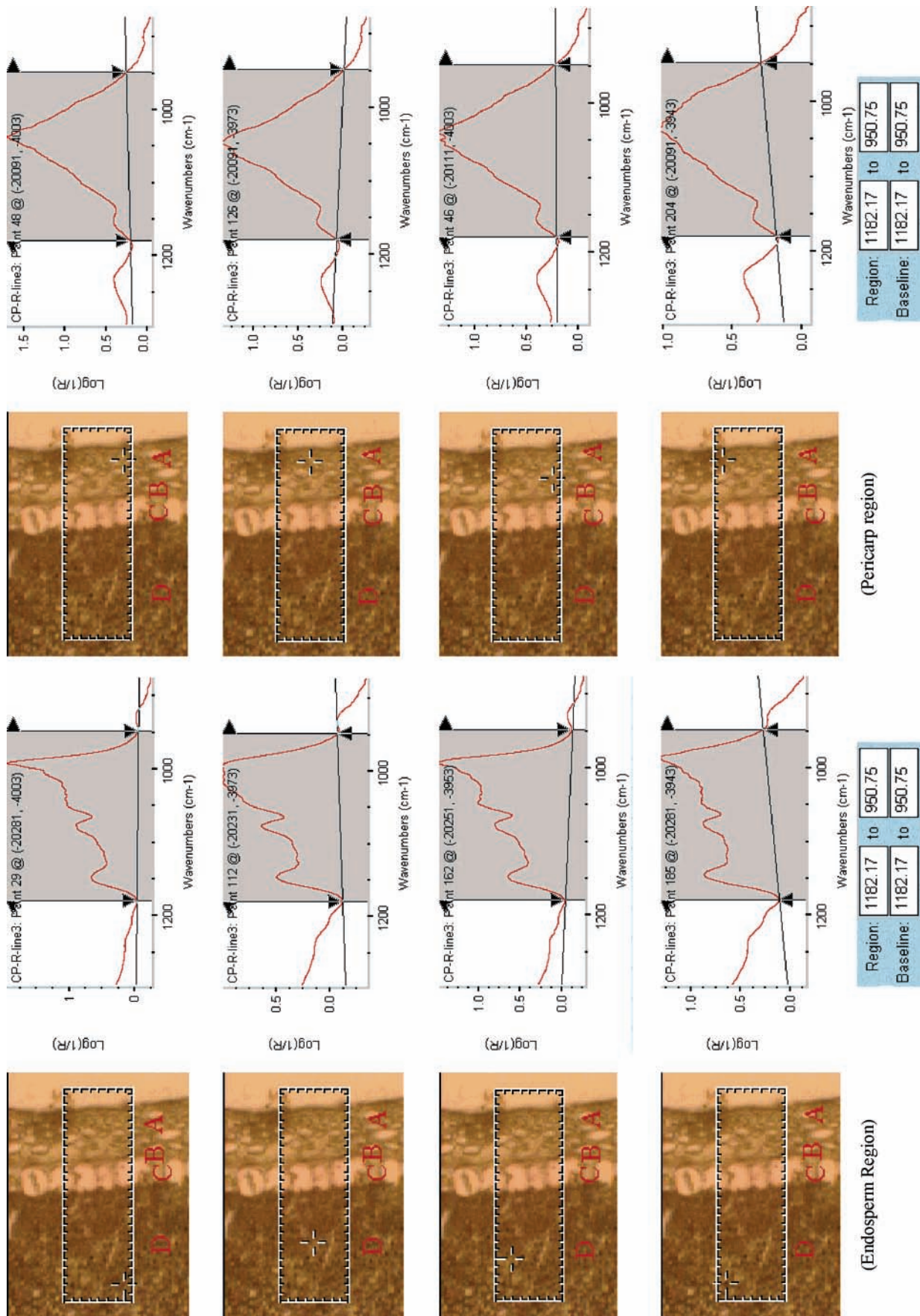


Figure 1. Spectra of pericarp (structural CHO) and endosperm (nonstructural CHO) of feed corn tissue selected from corresponding pixels from visible images, showing area under the $\sim 1180\text{--}950\text{ cm}^{-1}$ peak (CHO) for CHO intensities. Spectrum bands in the pericarp (left column) and endosperm (right column) regions are completely different, indicating that carbohydrate under the $1180\text{--}950\text{ cm}^{-1}$ peak does not distinguish structural and nonstructural carbohydrate intensity and distribution (A, pericarp; B, seed coat; C, aleurone; D, endosperm)

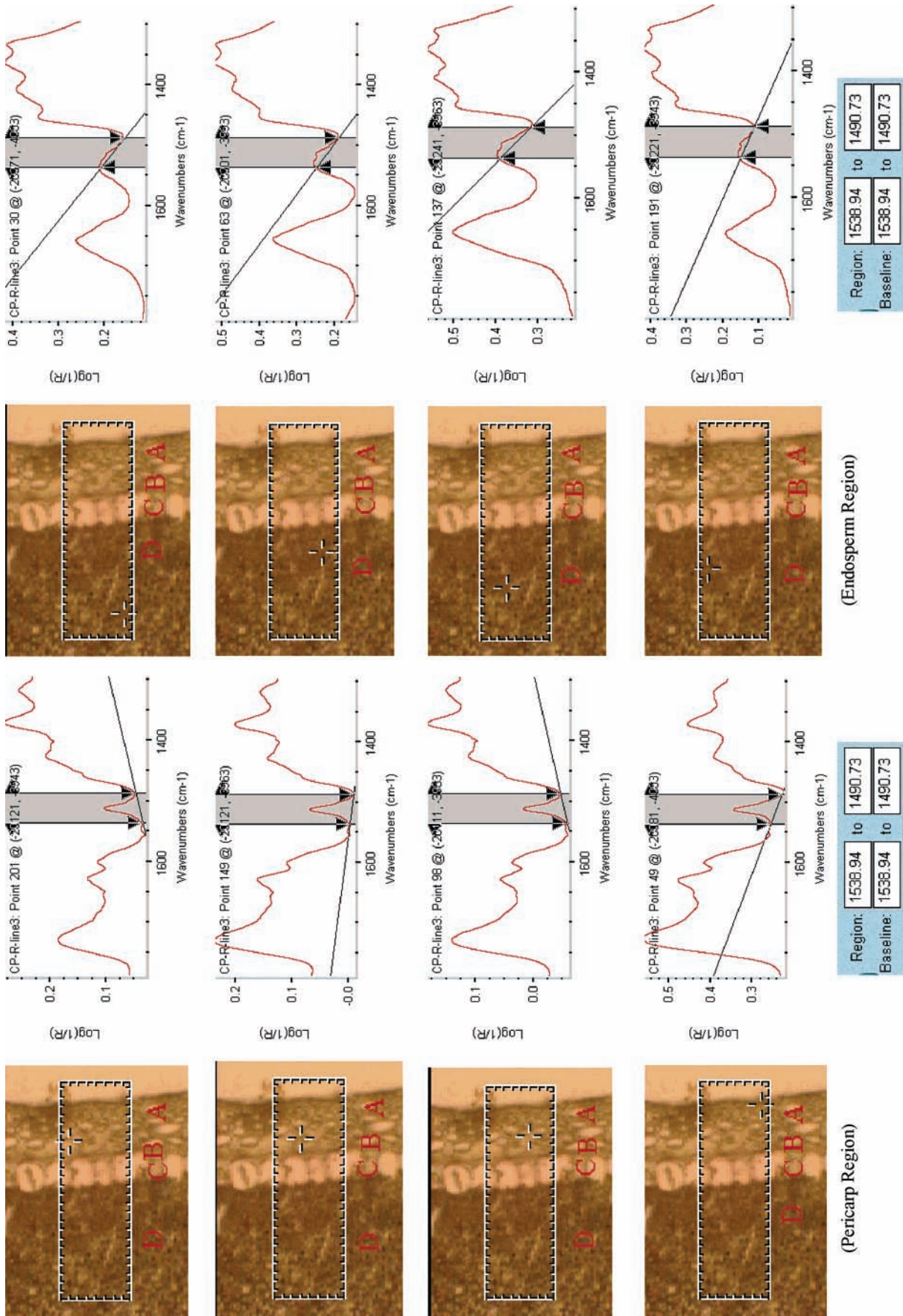
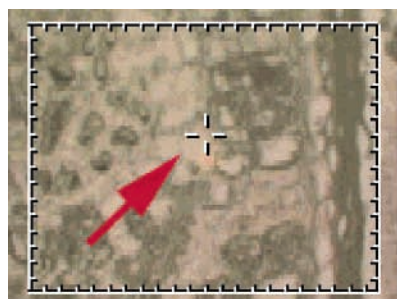
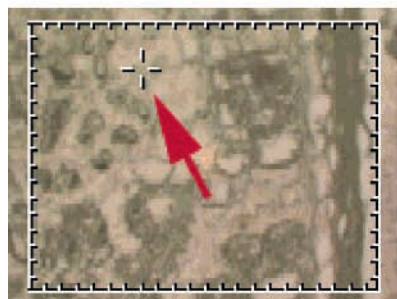


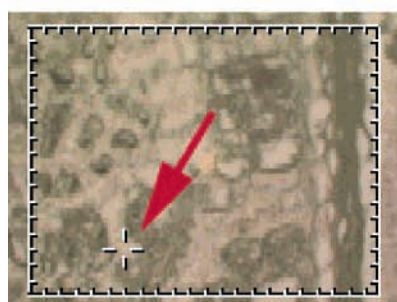
Figure 2. Spectra of pericarp (structural CHO) and endosperm (nonstructural CHO) of corn tissue selected from corresponding pixels from visible images, showing area under the $\sim 1515\text{ cm}^{-1}$ peak (aromatic compound) in the pericarp for lignin intensities (left spectrum) covering part of the amide I band in the endosperm (right spectrum), indicating that lignin under the $\sim 1515\text{ cm}^{-1}$ peak has interference with part of the amide I band and thus does not accurately represent lignin intensity and distribution in the tissue.



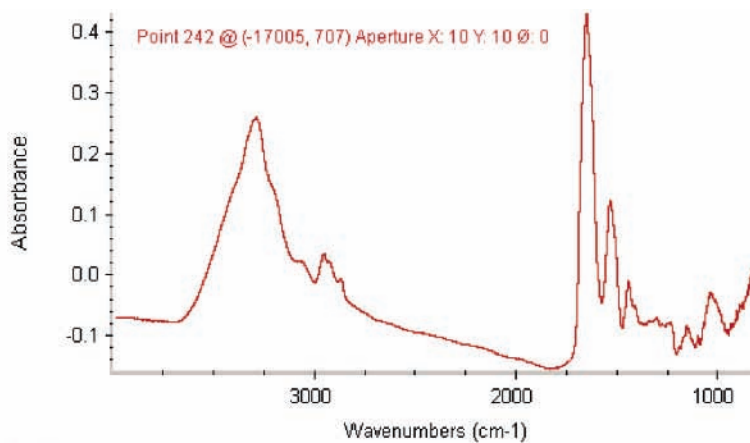
B_E1 (pixel-242 in endosperm)



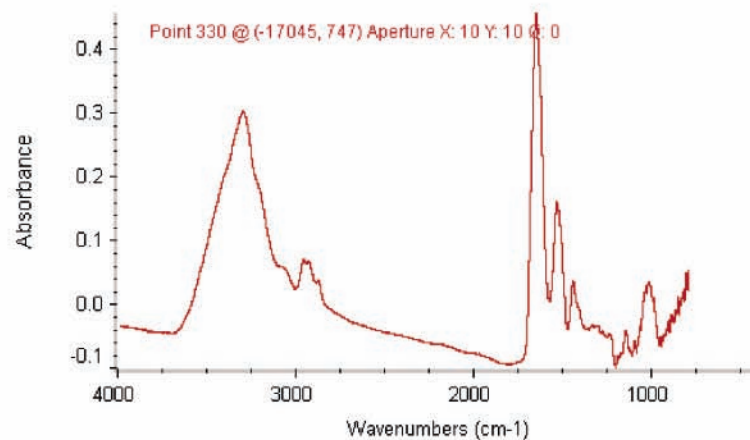
B_E2 (pixel-330 in endosperm)



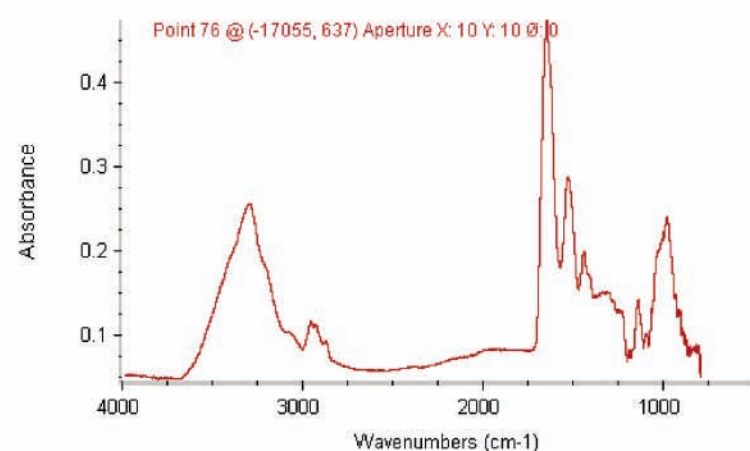
B_E3 (pixel-76 in endosperm)



B_E1 spectrum



B_E2 spectrum



B_E3 spectrum

Figure 3. Structural infrared spectra of endosperm of barley seed tissue selected from corresponding area from visible images, showing that similar morphological parts exhibit similar spectral characteristics.

varieties of feeds using synchrotron FTIR microspectroscopy to reveal structural–chemical features at cellular and subcellular levels within intact tissues and to illustrate the importance of CLA and PCA in the feed microstructural analysis, which could be used to discriminate and classify inherent structures between and among feed structures and feed molecular chemistry.

MATERIALS AND METHODS

Selected Feed Tissues. Feed-type grain barley (Valier), grown in a university research plot near Saskatoon (Canada), was supplied by the Crop Development Center (CDC), University of Saskatchewan (Saska-

toon, SK, Canada). Grain corn (cv. Pioneer 39P78) at harvest maturity was obtained from Henry Penner (Morden, MB, Canada), which was arranged by the Prairie Feed Resource Centre (Canada) (Director, Vern Racz). The yellow-seeded (*Brassica rapa* cv. Klondike) (C1) and dark brown-seeded (*Brassica napus* cv. Bounty) (C2) canolas were supplied by R. W. Newkirk, Department of Animal and Poultry Science, University of Saskatchewan (Saskatoon, SK, Canada). Raw and roasted golden and brown flaxseeds were obtained from CanMar Grain Products Ltd. (Regina, SK, Canada).

Synchrotron FTIR Slide and Window Preparation. The feed samples were cut into thin cross sections ($\sim 6 \mu\text{m}$ thick) at the Western College of Veterinary Medicine, University of Saskatchewan (Saska-

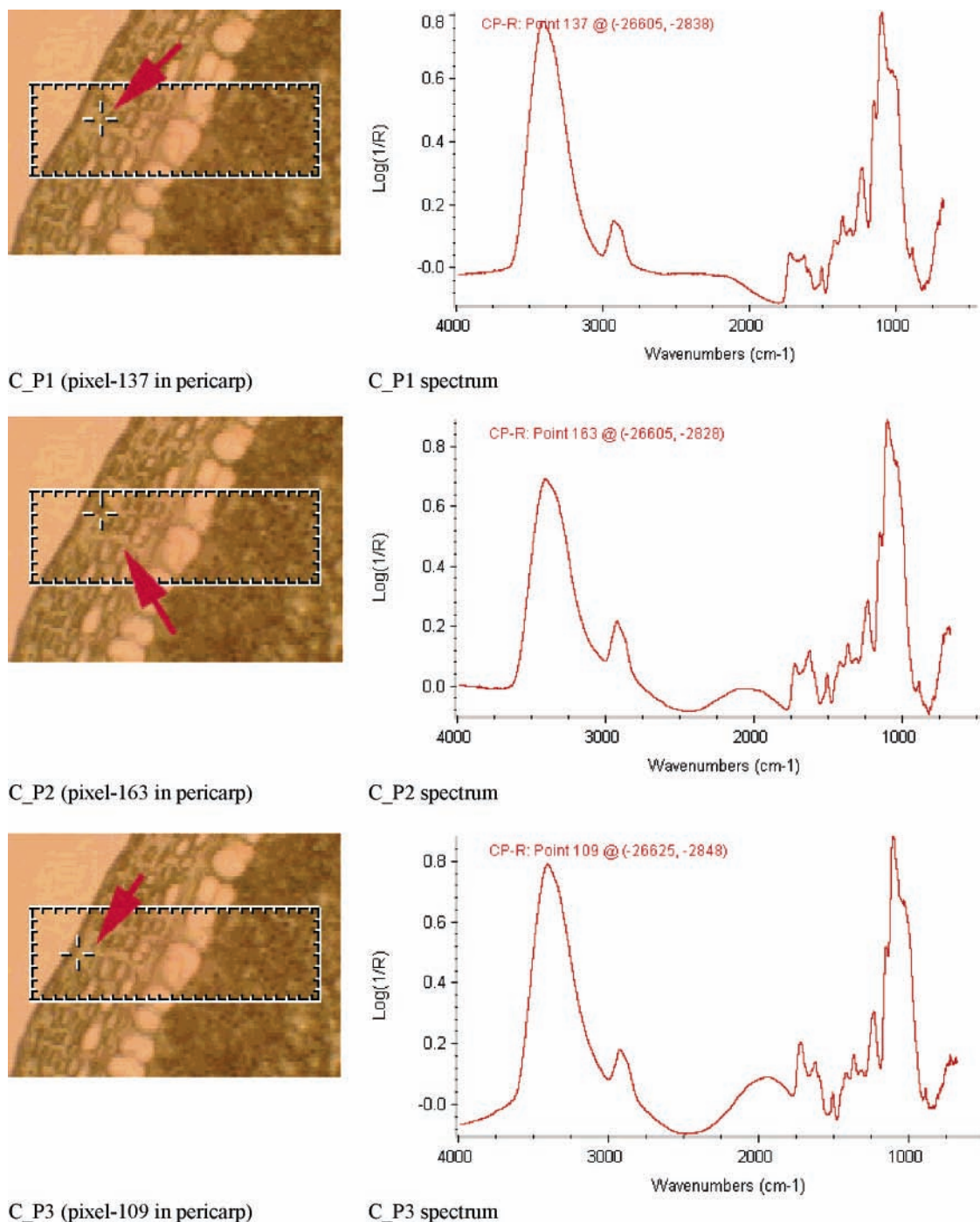


Figure 4. Structural infrared spectra of pericarp (structural CHO) of the Pioneer corn tissues selected from corresponding area from visible images, showing that similar morphological parts exhibit similar spectral characteristics.

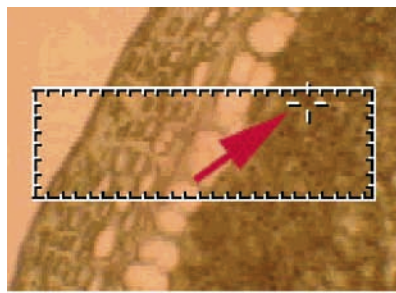
toon, Canada). The unstained cross sections were mounted onto low-e IR microscope slides (Kevley Technologies, Chesterland, OH) or BaF₂ windows (size, 13 × 1 mm disk; part no. 915-3015, Spectral Systems, New York) for synchrotron FTIR microspectroscopy work.

Synchrotron Light Source and Synchrotron FTIR Microspectroscopy. The experiment was carried out at the National Synchrotron Light Source at Brookhaven National Laboratory (NSLS-BNL, New York). The beamline is equipped with a FTIR spectrometer (Nicolet Magna 860) with a KBr beam splitter and an MCT-A detector coupled with an IR microscope (Nic-Plan, Nicolet Instruments, Madison, WI). The bench was configured to use collimated synchrotron light (beam energy = 800 MeV) through an external input of the spectrometer. The modulated light was passed through the Nic-Plan IR microscope to perform reflection microscopy. The IR spectra were collected in the mid-IR range of 4000–800 cm⁻¹ at a resolution of 4 cm⁻¹ with 64 scans co-added and an aperture setting of ca. 10 μm × 10 μm. The

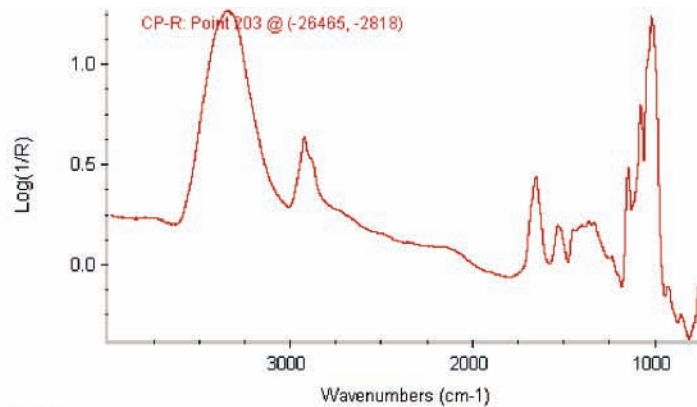
aperture size of 10 μm × 10 μm was chosen because (1) the size was within cellular dimensions and (2) the 10 × 10 μm aperture size was the best for getting a good signal-to-noise ratio spectrum. To minimize IR absorption by CO₂ and water vapor in ambient air, the optics were purged using dry N₂. A background spectroscopic image file was collected from an area free of sample. The mapping steps were equal to aperture size. Stage control, data collection, and processing were performed using OMNIC 6.0 (Thermo-Nicolet, Madison, WI).

Spectral Data Analysis. The S-FTIR spectral data of the feed tissues were collected, corrected for the background spectrum, and analyzed using OMNIC software 6.0 (Thermo-Nicolet). The data can be displayed as a collection of S-FTIR spectra obtained at each pixel position in the image. The Fourier self-deconvolution (FSD) spectra were obtained using the OMNIC.

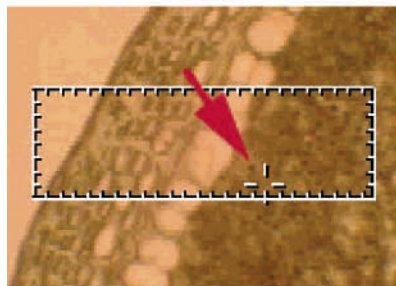
Multivariate Statistical Analysis for Synchrotron-Based FTIR Spectra. Multivariate analyses, CLA and PCA, were performed using



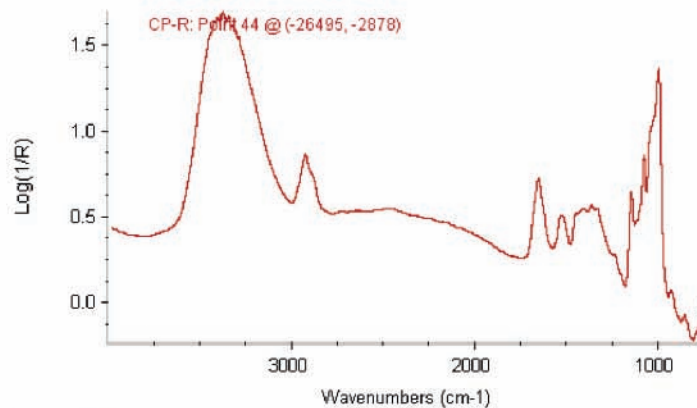
C_E1 (pixel-203 in aleurone)



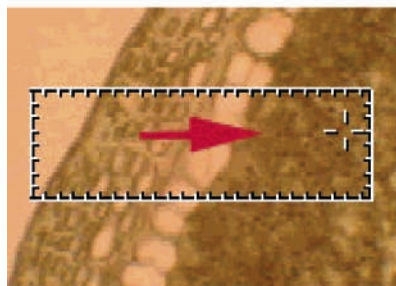
C_E1 spectrum



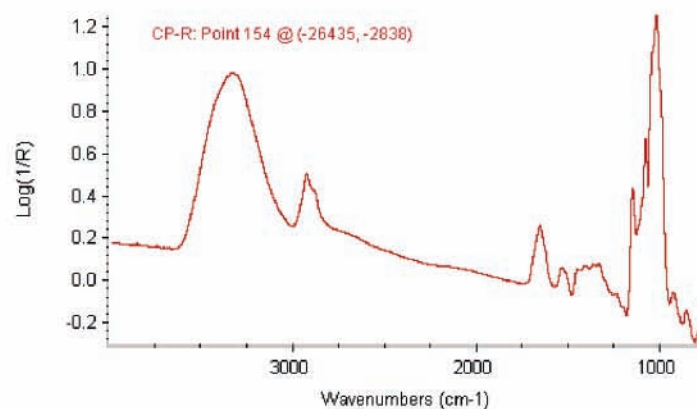
C_E2 (pixel-44 in aleurone)



C_E2 spectrum



C_E3 (pixel-154 in aleurone)



C_E3 spectrum

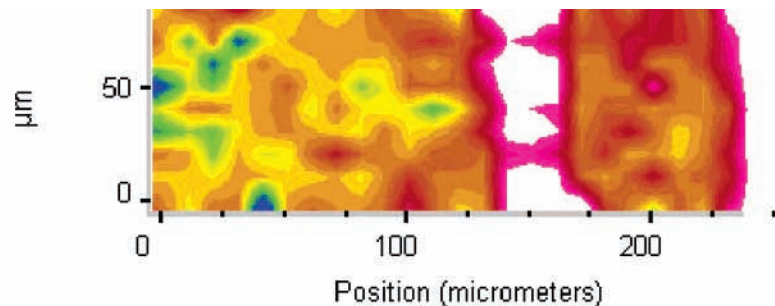
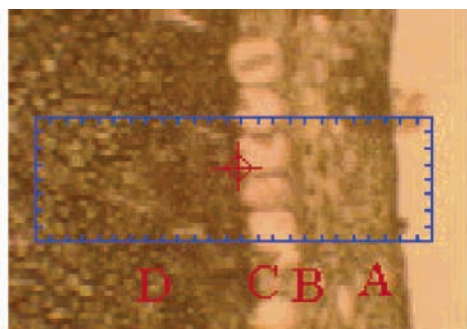
Figure 5. Structural infrared spectra of aleurone of Pioneer corn tissues selected from corresponding area from visible images, showing that similar morphological parts exhibit similar spectral characteristics and chemical composition.

Statistica software 6.0 (StatSoft Inc., Tulsa, OK) to classify the feed inherent microstructures, which are associated with digestive behaviors and nutrient utilization.

Cluster Analysis. The first multivariate analysis is CLA, which performs an agglomerative hierarchical cluster analysis of an IR spectral data set and displays the results of CLA as dendrograms. First, it calculates the distance matrix, which contains information on the similarity of spectra. Then, in hierarchical clustering, the algorithm searches within the distance matrix for the two most similar IR spectra (minimal distance). These spectra are combined into a new object (called a "cluster" or called "hierarchical group"). The spectral distances between all remaining spectra and the new cluster are recalculated (16). It is a technique that clusters IR spectra on the basis of similarity with other spectra.

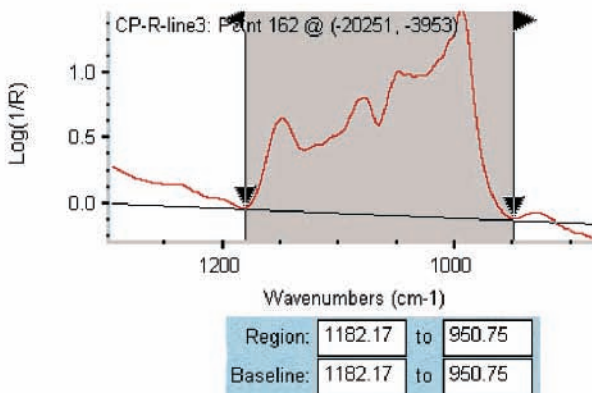
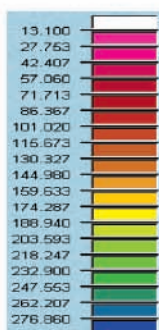
Principal Component Analysis. The second multivariate analysis is PCA, which is a statistical data reduction method. It transforms the original set of variables to a new set of uncorrelated variables called

principal components (PCs). The first few PCs will typically account for >95% of the variance. The purpose of PCA is to derive a small number of independent linear combinations (PCs) of a set of variables that retain as much of the information in the original variables as possible. This analysis allows global study of the relationships between p quantitative characters (e.g., feed chemical functional groups) observed on n samples (e.g., FTIR spectra of feeds and feed structures). The basic idea is to extract, in a multiple-variable system, one, two, or sometimes more PCs that carry maximum information. These components are independent (orthogonal) of each other, and the first factor generally represents maximum variance. As factors are extracted, they account for less and less variability, and the decision of when to stop basically depends on the point when there is only very little significant variability or merely random noise left. Thus, reduction of data provides a new coordinate system wherein axes (eigenvectors) represent the characteristic structure information of the data, and the spectra may then be simply described as function of specific properties and no longer



1. Visible image
(The rectangle area size: 250 μm \times 80 μm)

2 Chemical image-CHO



3. Chemical intensity ruler

4. Functional group -CHO band and mapping region and baseline

Figure 6. Carbohydrate image of Pioneer corn tissue from the pericarp (A, in visible image), seed coat (B), aleurone (C), and endosperm (D): area under the area under the 1180–950 cm^{-1} peak (CHO C–O stretching) peak with mapping region and baseline 1182–950 cm^{-1} .

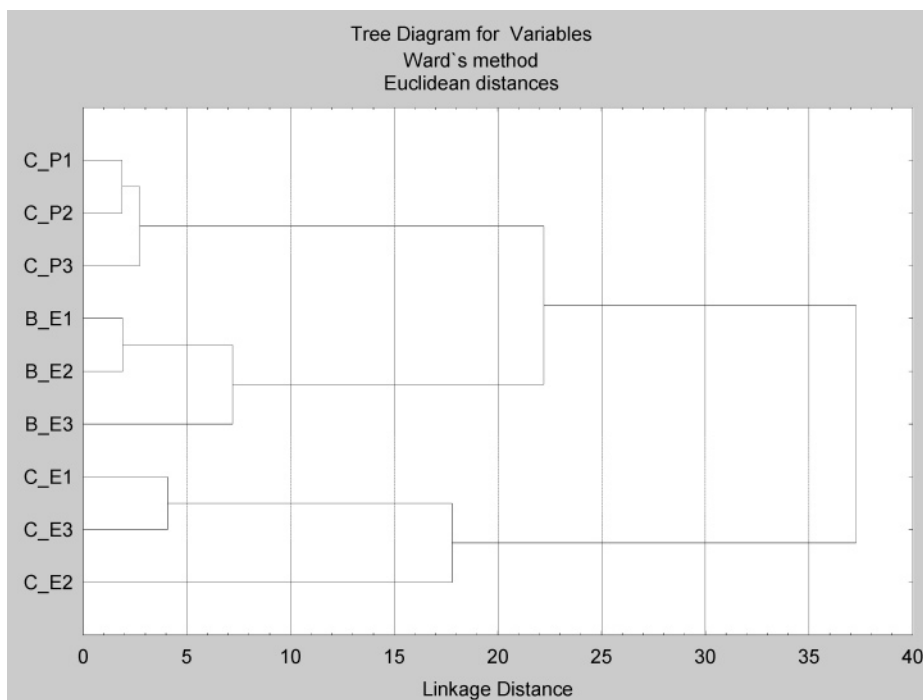


Figure 7. CLA cluster of feed intrinsic structures showing that the clusters in the pericarp region, aleurone layer, and endosperm region are different between feeds and between feed structures within the feed [CLA analysis: (1) select spectral region, 4000–800 cm^{-1} ; (2) distance method, Euclidean; (3) cluster method, Ward's algorithm].

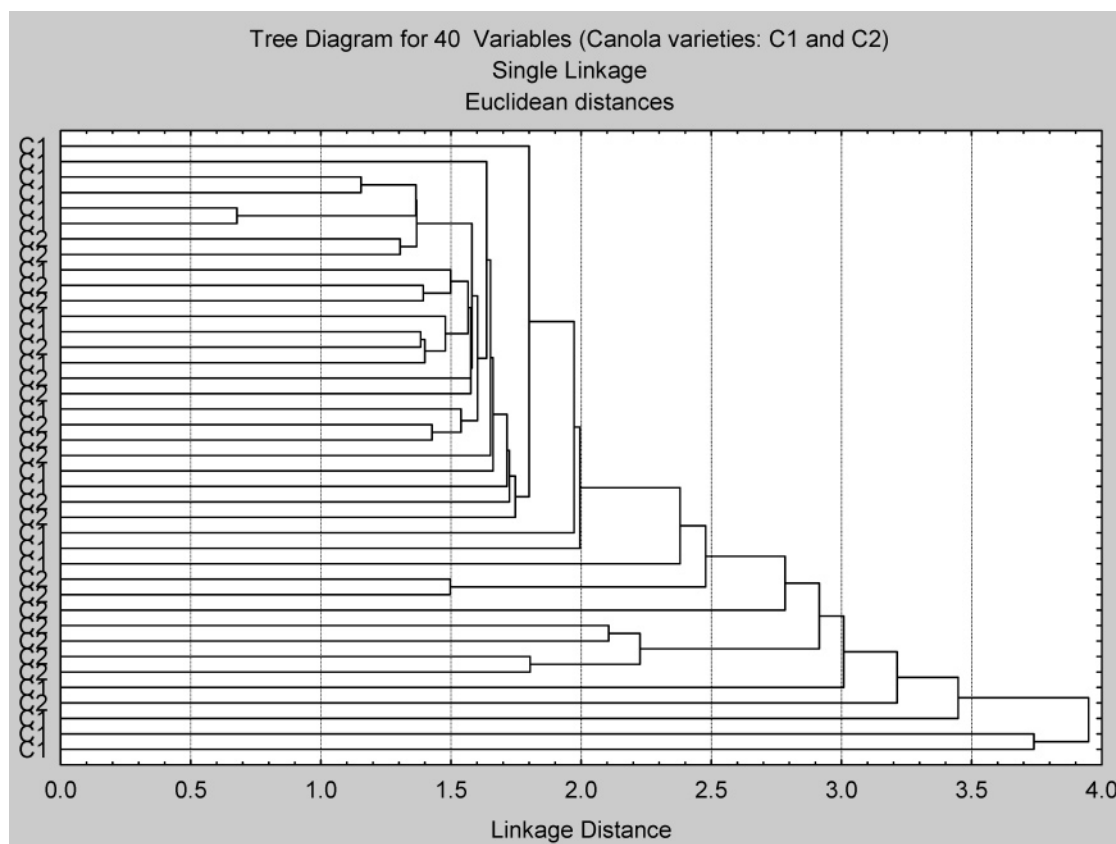


Figure 8. CLA cluster of synchrotron-based protein amide I FSD spectrum obtained from the canola seed tissues at a cellular level (pixel size, $10 \mu\text{m} \times 10 \mu\text{m}$): C1, yellow-seeded (*Brassica rapa*); C2, brown-seeded (*Brassica napus*) canola (total sample number for each variety = 20) [CLA analysis: (1) FSD spectral region, $1710\text{--}1576 \text{ cm}^{-1}$; (2) distance method, Euclidean; (3) cluster method, Ward's algorithm].

as a function of intensities. The outcome of such an analysis can be presented as either two-dimensional (2D) (two PCs) or three-dimensional (3D) (three PCs) scatter plots (17).

RESULTS AND DISCUSSION

Univariate and Multivariate Statistical Approaches for Spectrum Analysis. Statistical approaches to the analysis of spectral data collected under synchrotron FTIR microspectroscopy usually include uni- and multivariate statistical methods. The univariate methods of analysis consist of various mapping (e.g., area mapping, line mapping, and spot mapping) displays of spectral data. Usually, researchers may select band intensities, integrated intensities, band frequencies, band intensity ratios, etc., to construct color maps of the spectral data (13, 15). For example, feed ultrastructural chemical mapping (6, 9). The multivariate methods of data analysis create spectral corrections by utilizing the entire spectral information. The analysis methods include CLA and PCA (13).

Univariate Statistical Analysis Fails To Discriminate and Classify Inherent Structures of Feeds. Analysis of absorbance peak height and/or areas provides a measure of component concentration and distribution. Provided that individual components can be uniquely identified, measuring peak height and/or areas is the most straightforward way of identifying its location and concentration (13). However, this univariate statistical approach is not always accurate to identify chemical functional group location and concentration even when individual components are uniquely identified, particularly when different functional group spectra are in the same IR region but show different band patterns. For example, structural carbohydrate (cellulose, hemicellulose) and nonstructural carbohydrate

(starch) in feed tissues both show a peak at the $\sim 1180\text{--}950 \text{ cm}^{-1}$ region (3). It is almost impossible to distinguish the two types of carbohydrates by the univariate statistical analysis using peak heights and/or areas as shown in **Figure 1**. Himmelsbach et al. (18) reported that the band at 1515 cm^{-1} shows no interference with any other bands and, thus, it is an ideal diagnostic band for aromatics of lignin. However, our study showed that the lignin band under the $\sim 1515 \text{ cm}^{-1}$ peak has more or less interference with part of the amide I band and thus does not precisely represent lignin intensity and distribution in the feed tissue (**Figure 2**).

Figures 3–5 show three feed structural IR spectra data sets between feeds of different structures; however, similar morphological parts exhibit similar spectral characteristics. The major absorptions from carbohydrates are found in the $1180\text{--}950 \text{ cm}^{-1}$ region of the spectrum and are attributed to C–O and C–C stretching vibrations and C–O–H deformation. **Figure 6** is a chemical image under the area at $1182\text{--}950 \text{ cm}^{-1}$ showing the total carbohydrates spatial distribution. Usually, carbohydrates in a feed consist of structural and nonstructural carbohydrates. Carbohydrate band mapping as shown in **Figure 6** could not distinguish the types of carbohydrates (structural versus nonstructural). **Figure 1** clearly shows that the carbohydrate band in the endosperm region (see the left side of **Figure 1**) is completely different from the pericarp region (see the right side of **Figure 1**), indicating that the carbohydrate image under the $1180\text{--}950 \text{ cm}^{-1}$ peak cannot distinguish structural and nonstructural carbohydrates.

Multivariate Statistical Analyses Are Able To Discriminate and Classify Inherent Structures of the Feeds. *Cluster Analysis for Feed Intrinsic Structure.* The first multivariate

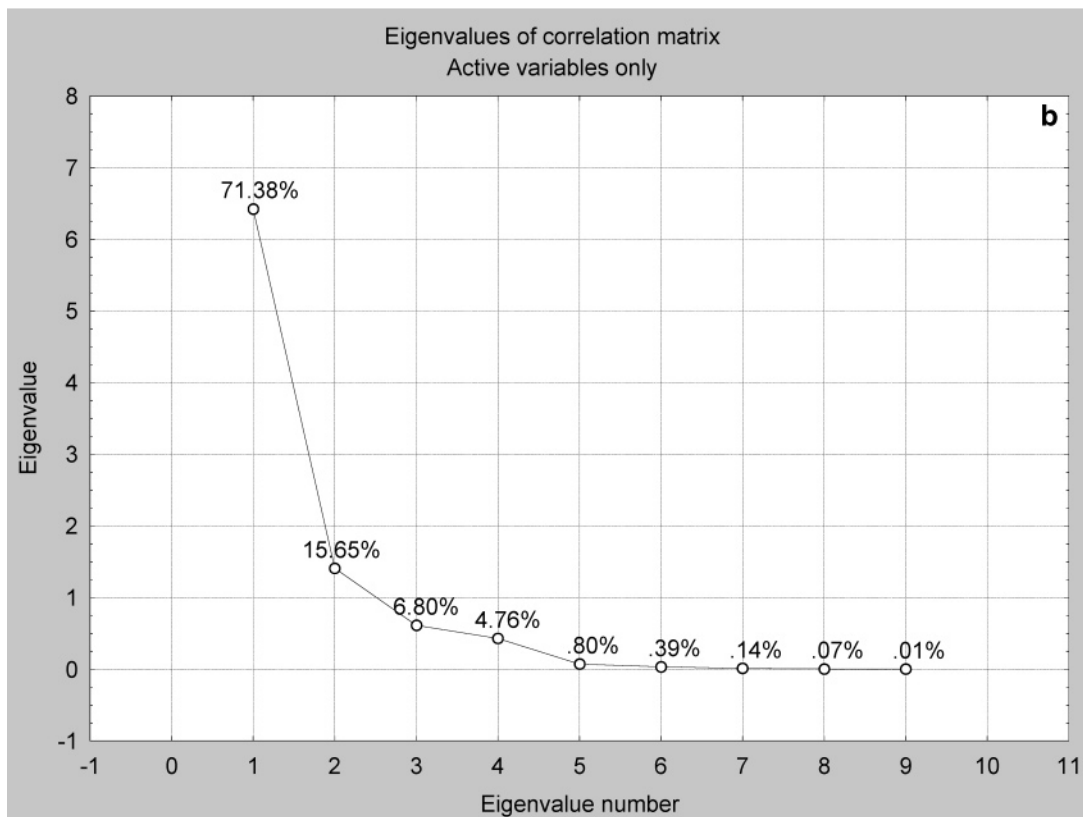
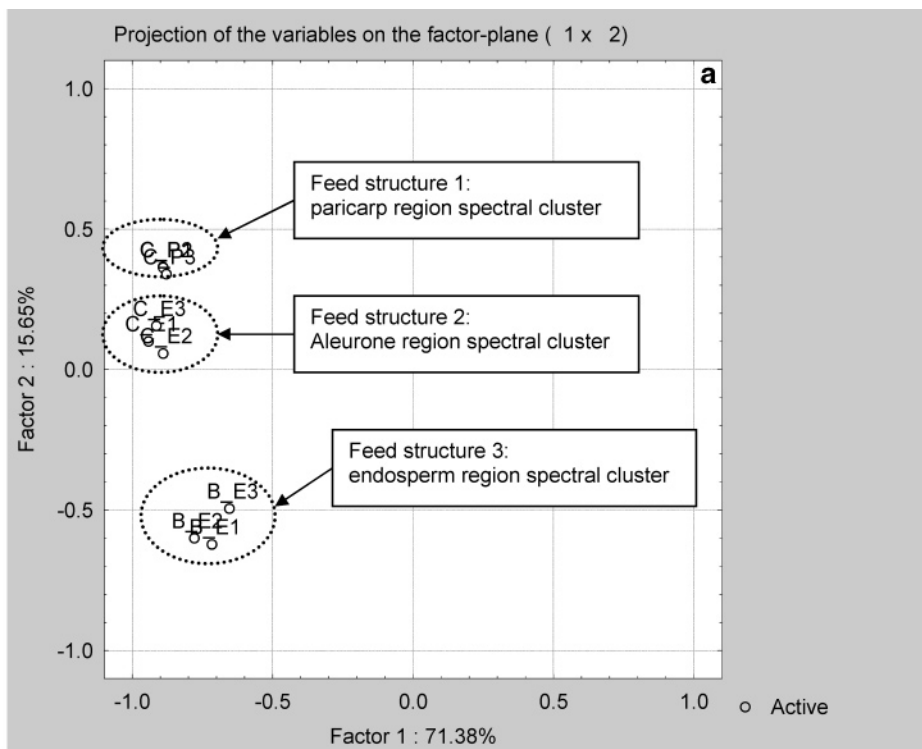
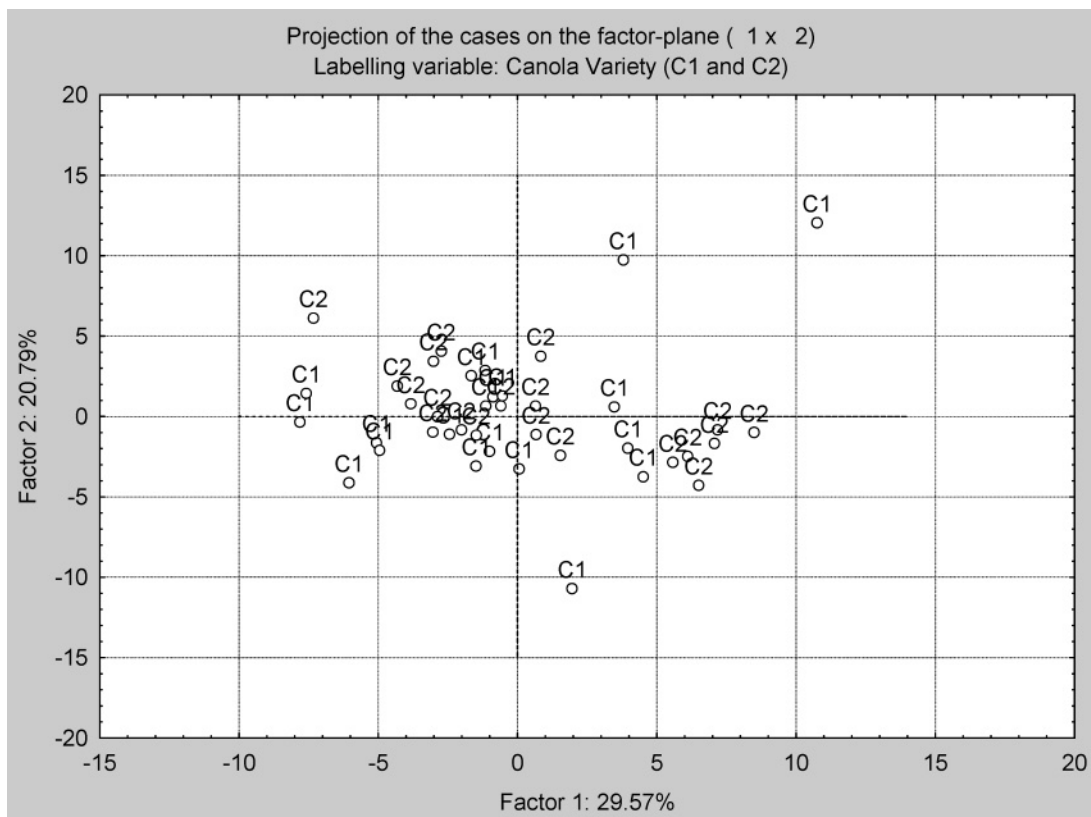
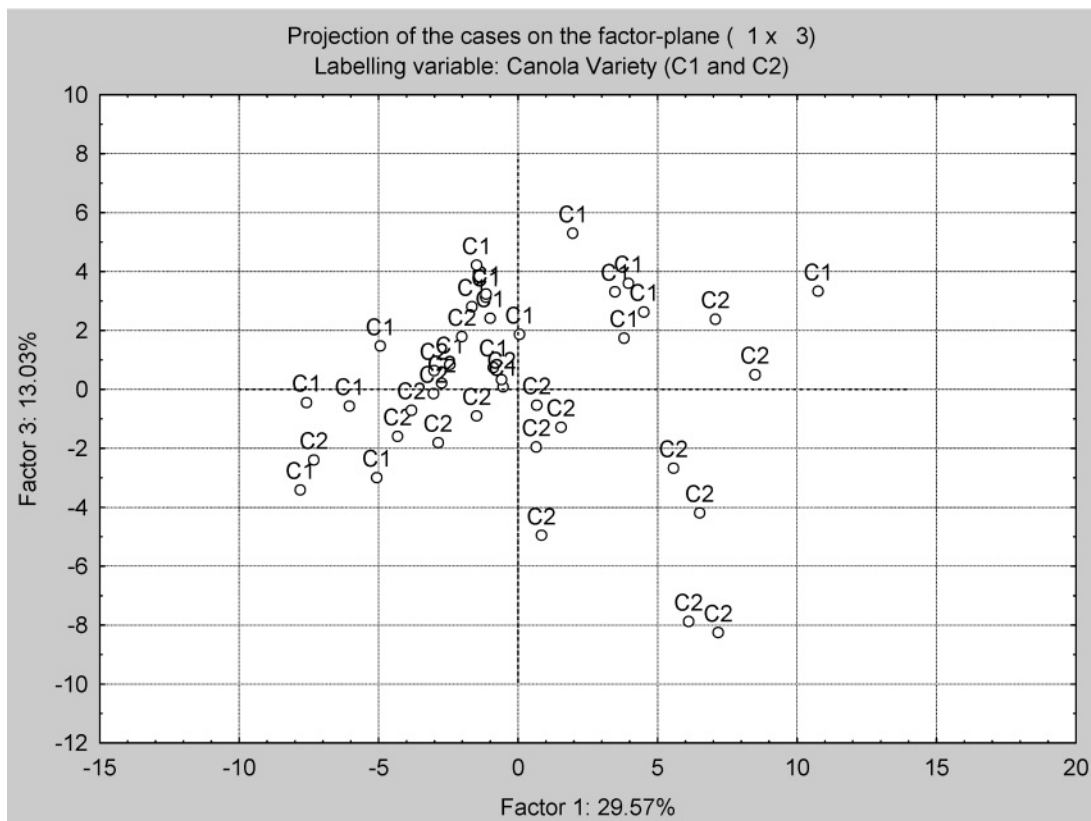


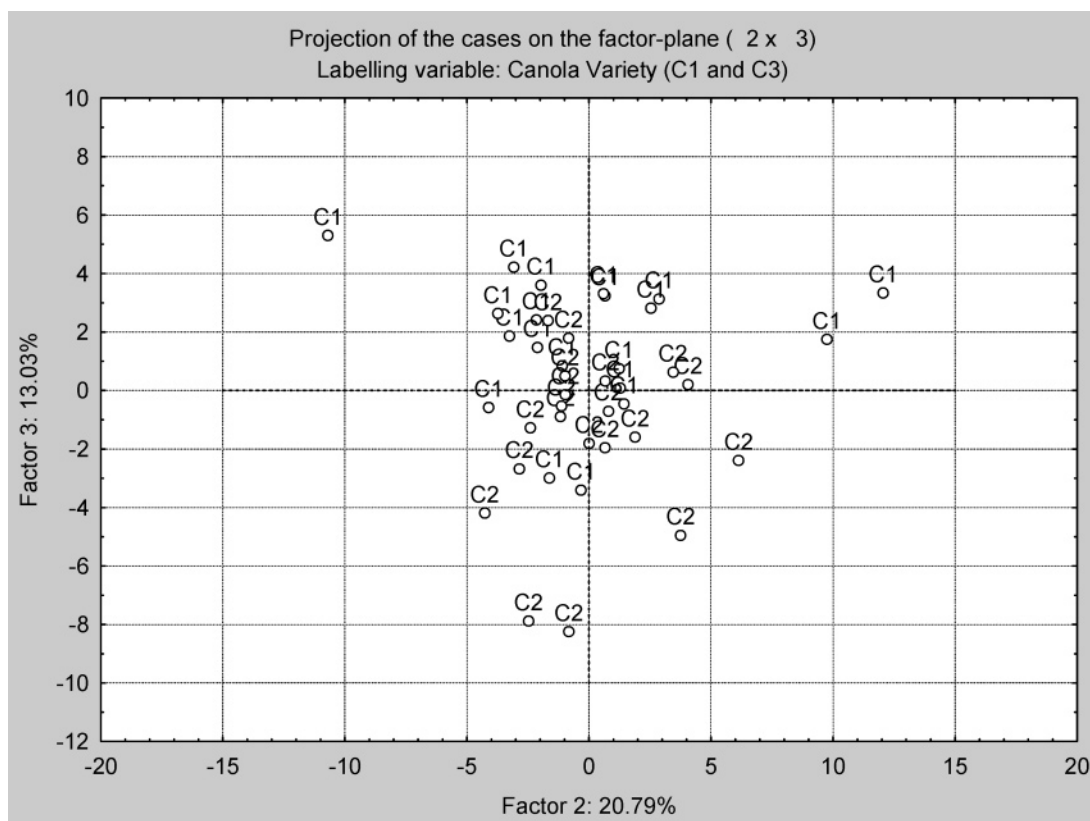
Figure 9. (a) PCA of synchrotron-based FTIR spectrum obtained from various feed intrinsic structures within intact tissue at a cellular level: scatter plot of the first principal component versus the second principal components (top ellipse, feed structure 1 = pericarp; middle ellipse, feed structure 2 = aleurone; bottom ellipse, feed structure 3 = endosperm), showing separation of feed IR spectra generated by the covariance–matrix approach for PCA. Feed structures 1–3 form three distinguishable populations, indicating that PCA distinguishes the feed structural differences in the pericarp region, aleurone layer, and endosperm region between the feeds and between the structures within the feed. The first principal component explains 71% of the variance, whereas the second principal component explains 17% of the variance. (b) Eigenvalue of PCA of synchrotron-based IR spectrum obtained from feed intrinsic structures within intact tissue at a cellular level. The first three principal components explain 71.4, 16.7, and 6.8% of the variation in the full data set, respectively.



(a) PCA Component 1 vs. PCA Component 2



(b) PCA Component 1 vs. PCA Component 3



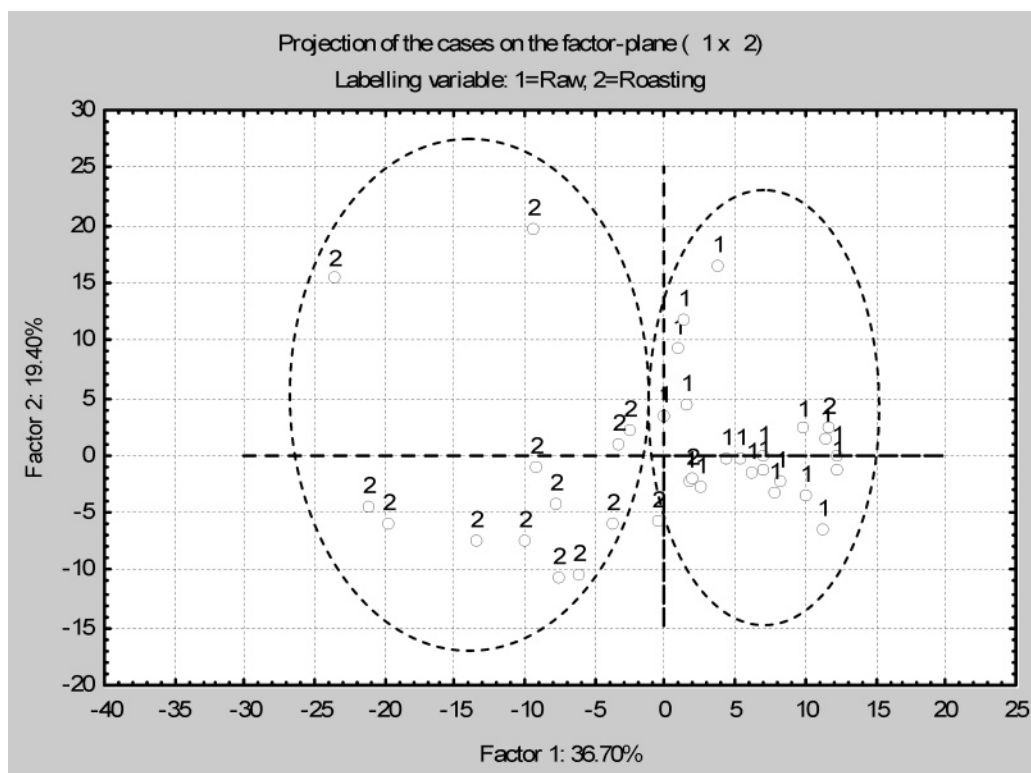
(c) PCA Component 2 vs. Component 3

Figure 10. PCA of synchrotron-based protein FSD amide I spectrum obtained from canola seed tissue at a cellular level (pixel size, $10\ \mu\text{m} \times 10\ \mu\text{m}$) [C1, yellow-seeded (*Brassica rapa*); C2, brown-seeded (*Brassica napus*) canola (total sample number for each variety = 20)]: (a) scatter plot of the first principal component versus the second principal component; (b) scatter plot of the first principal component versus the third principal component; (c) scatter plot of the second principal component versus the third principal component. (The first principal component explains 30% of the variance, whereas the second principal component explains 21% of the variance and the third principal component explains 13% of the variance.)

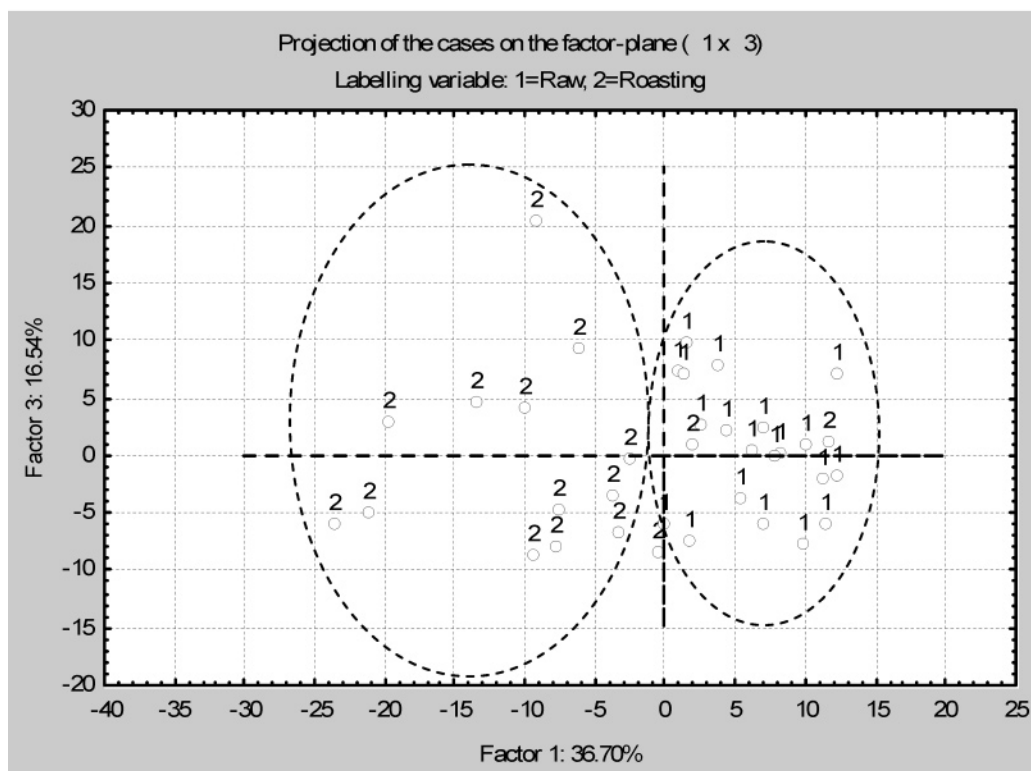
analysis is CLA. It is a technique that clusters IR spectra on the basis of similarity with other spectra. In this study, Ward's algorithm method was used without any prior parametrization of the spectral data (original spectral data were used) in the IR region ($4000\text{--}800\ \text{cm}^{-1}$). This method gave good results with a better discrimination of different feed structures. **Figure 7** displays the results in the form of a dendrogram. From this diagram, three classes can be distinguished below a linkage distance of <23 , with the C-E group forming a separate group. Depending on the aggregation level (horizontal axis) different explanations can be inferred. The C_P and B_E groups form two distinct groups just below an aggregation (linkage) distance of 8. They form a single group at an aggregation distance of ~ 22 . The C_E group can be grouped together with the C_P and B_E groups for a linkage distance equal to ~ 38 . **Figure 7** clearly shows significantly different spectral clusters in the different feed structures: pericarp region, aleurone layer, and endosperm region using the whole spectral region from 4000 to $800\ \text{cm}^{-1}$ for CLA. In other words, different feed structures have different spectral clusters, and different feeds have different spectral clusters. **Figure 8** is another example showing the results in the form of a dendrogram from CLA for feed protein amide I in the yellow- and brown-seeded canola tissues. From this diagram, the two varieties of canola seed were not distinguished from each other in protein amide I structures.

Principal Component Analysis for Feed Intrinsic Structure. The second multivariate analysis is PCA, which is a statistical data reduction method. In this feed intrinsic structure study, PCA was used to identify the main sources of variation in the synchrotron FTIR spectra in the region of $4000\text{--}800\ \text{cm}^{-1}$ of

different feed structures (pericarp, aleurone, endosperm) at a cellular level and to identify features that differ between feed microstructures. **Figure 9** show results from PCA of the synchrotron FTIR data obtained from different feed microstructures. The first two PCs (obtained after data reduction) were plotted (**Figure 9a**), showing that three feed structures can be grouped in separate ellipses and that there is no overlapping of each group. **Figure 9b** shows that the first three PCs explain 71.4, 16.7, and 6.8% of the variation, respectively, in the full synchrotron FTIR data set. The scores scatter plot shown in **Figure 9a** allows the distinction between feed structures along the first PC axis, which corresponds to nearly 71% of the variability contained in the FTIR spectra, whereas the second PC explains 17% of the variance. Therefore, this PCA allows the feed intrinsic structures to be distinguished and identifies features that differ between feed structures. **Figure 10** is another example showing the results from PCA of the spectrum data—the synchrotron-based protein amide I FSD spectra in the region of $1710\text{--}1576\ \text{cm}^{-1}$ —obtained from two different canola seed structures (the yellow- versus brown-seeded canola tissues). The first three PCs (obtained after data reduction) were plotted (**Figure 10**), showing that the two varieties of canola seed inherent protein structures cannot be grouped in separate ellipses because of overlapping of each group. **Figure 10** shows that the first three PCs explain 30, 21, and 13% of the variation, respectively, in the protein amide I FSD spectrum data set. Therefore, the PCA did not fully distinguish between the yellow- and brown-seeded canola tissues in protein amide I structures, indicating similarity in protein structures.



(a) PCA Component 1 vs. PCA Component 2



(b) PCA Component 1 vs. PCA Component 3

Figure 11. PCA of synchrotron-based protein FSD amide I spectrum ($1700\text{--}1620\text{ cm}^{-1}$) obtained from raw and roasted flaxseed tissues at a cellular level [1, raw flaxseed; 2, roasted flaxseed]: (a) scatter plot of the first principal component versus the second principal component; (b) scatter plot of the first principal component versus the third principal component. (The first principal component explains 36.7% of the variance, whereas the second principal component explains 19.4% of the variance and the third principal component explains 16.5% of the variance.)

In the study on the effect of roasting on changes of flaxseed protein inherent structure, PCA was used to identify the main sources of variation in the synchrotron-based protein amide I FSD spectra of the raw and roasted brown and golden flaxseed.

Figure 11 shows that PCA could almost fully distinguish between the raw and roasted flaxseeds in the protein amide I FSD spectrum and that the raw and roasted flaxseed can be grouped in separate ellipses. The first three PCs explain 36.7,

19.4, and 16.5% of the variation, respectively, in the protein amide FSD spectrum data set.

CONCLUSIONS AND IMPLICATIONS

Synchrotron FTIR microspectroscopy was capable of exploring the molecular chemistry within microstructures of feed tissues within cellular dimensions. Both PCA and CLA methods gave satisfactory results and are conclusive in showing that they can discriminate and classify inherent structures between feed structures, which are highly associated with feed quality and nutritive value and digestive behaviors in animals. They also can be used to identify whether feed varieties exhibit differences in microstructure. These analyses place synchrotron-based FTIR microspectroscopy at the forefront of those new potential techniques that could be used in rapid, nondestructive, and noninvasive screening of feed structures in relation to the quality and nutritive value of feeds. The implication from this study is that we can distinguish the structure difference between feeds and between feed inherent structures within a feed with PCA and CLA. Information on the structural–chemical features within the feed tissue can be used for plant breeding programs to select superior varieties of feed for special purposes and to predict feed quality and nutritive value.

ACKNOWLEDGMENT

I am grateful to L. M. Miller and N. S. Marinkovic (NSLS-BNL, New York) for helpful data collection at NSLS, M. Jackson (Institute for Biodiagnostics, National Research Council, Winnipeg, Canada) and C. R. Christensen (CLS, Canada) for helpful discussion, J. J. McKinnon and D. A. Christensen (University of Saskatchewan, Canada) for feed project support, K. M. Gough (University of Manitoba) for helpful discussion, and V. J. Racz (Prairie Feed Resource Centre), B. Rosnagel (Crop Development Center, Canada), and R. W. Newkirk (University of Saskatchewan, Canada; currently at Feed Section, Canadian International Grains Institute) for supplying feed samples.

LITERATURE CITED

- (1) Synchrotron facts, available at <http://www.cls.usask.ca/education/whatis.php>, accessed October 2004.
- (2) Miller, L. M.; Carlson, C. S.; Carr, G. L.; Chance, M. R. A method for examining the chemical basis for bone disease: synchrotron infrared microspectroscopy. *Cell. Mol. Biol.* **1998**, *44*, 117–127.
- (3) Wetzel, D. L.; Eilert, A. J.; Pietrzak, L. N.; Miller, S. S.; Sweat, J. A. Ultraspatially resolved synchrotron infrared microspectroscopy of plant tissue in situ. *Cell. Mol. Biol.* **1998**, *44*, 145–167.
- (4) Marinkovic, N. S.; Huang, R.; Bromberg, P.; Sullivan, M.; Toomey, J.; Miller, L. M.; Sperber, E.; Moshe, S.; Jones, K. W.; Chouparova, E.; Lappi, S.; Franzen, S.; Chance, M. R. Center for Synchrotron Biosciences' U2B beamline: an international resource for biological infrared spectroscopy. *J. Synchrotron Radiat.* **2002**, *9*, 189–197.
- (5) Dumas, P. *Synchrotron IR Microspectroscopy: A Multidisciplinary Analytical Technique*; 6th Annual Synchrotron CLS Users' Meeting and Associated Synchrotron Workshops—WinXAS and Infrared; University of Saskatchewan: Canada, Nov 13–15, 2003.
- (6) Yu, P.; McKinnon, J. J.; Christensen, C. R.; Christensen, D. A.; Marinkovic, N. S.; Miller, L. M. Chemical imaging of microstructures of plant tissues within cellular dimension using synchrotron infrared microspectroscopy. *J. Agric. Food Chem.* **2003**, *51*, 6062–6067.
- (7) Yu, P. Application of advanced synchrotron-based Fourier transform infrared microspectroscopy (SR-FTIR) to animal nutrition and feed science: a novel approach. *Br. J. Nutr.* **2004**, *92*, 869–885.
- (8) Yu, P. Protein secondary structures (α -helix and β -sheet) at a cellular level and protein fractions in relation to rumen degradation behaviors of protein: a novel approach. *Br. J. Nutr.* **2005**, in press.
- (9) Yu, P.; McKinnon, J. J.; Christensen, C. R.; Christensen, D. A. Imaging molecular chemistry of Pioneer corn. *J. Agric. Food Chem.* **2004**, *52*, 7345–7352.
- (10) Yu, P.; McKinnon, J. J.; Christensen, C. R.; Christensen, D. A. Using synchrotron-based FTIR microspectroscopy to reveal chemical features of feather protein secondary structure: comparison with other feed protein sources. *J. Agric. Food Chem.* **2004**, *52*, 7353–7361.
- (11) Yu, P.; Christensen, D. A.; Christensen, C. R.; Drew, M. D.; Rosnagel, B. G.; McKinnon, J. J. Use of synchrotron FTIR microspectroscopy to identify chemical differences in barley endosperm tissue in relation to rumen degradation characteristics. *Can. J. Anim. Sci.* **2004**, *84*, 523–527.
- (12) Miller, L. M. The impact of infrared synchrotron radiation on biology: past, present, and future. *Synchrotron Radiat. News* **2000**, *13*, 31–37.
- (13) Miller, L. M. Infrared microspectroscopy and imaging; retrieved October 2002 from <http://nslsweb.nsls.bnl.gov/nsls/pubs/nslspubs/imaging0502/irxrayworkshopintroduction.ht>.
- (14) Budevskva, B. O. *Vib. Spectrosc.* **2002**, 3720–3732.
- (15) Jackson, M.; Mantsch, H. H. Infrared spectroscopy ex vivo tissue analysis. In *Encyclopedia of Analytical Chemistry*; Meyers, R. A., Ed.; Wiley: Chichester, U.K., 2000; pp 131–156.
- (16) Cytospec. Software for infrared spectral imaging, v. 1.1.01; 2004.
- (17) Sockalingum, G. D.; Bouhedja, W.; Pina, P.; Allouch, P.; Bloy, C.; Manfait, M. FT-IT spectroscopy as an emerging method for rapid characterization of microorganisms. *Cell. Mol. Biol.* **1998**, *44*, 261–269.
- (18) Himmelsbach, D. S.; Khalili, S.; Akin, D. E. FT-IR microspectroscopic imaging of flax (*Linum usitatissimum* L.) stems. *Cell. Mol. Biol.* **1998**, *44*, 99–108.

Received for review April 25, 2005. Revised manuscript received July 4, 2005. Accepted July 14, 2005. This research has been supported by grants from the Natural Sciences and Engineering Research Council of Canada (NSERC, Individual Discovery Grant) and the Saskatchewan Agricultural Development Fund (ADF). The National Synchrotron Light Source at Brookhaven National Laboratory (NSLS-BNL, New York) is supported by U.S. Department of Energy Contract DE-AC02-98CH10886.

JF050959B